

Original Research

Small Extracellular Vesicles Promote HBV Replication via METTL3–IGF2BP2-Mediated m6A Modification

Jie Zhang¹, Ling Yu², Xinyu Wu¹, Wanlong Pan^{1,*}

Academic Editor: Giuseppe Murdaca

Submitted: 11 December 2024 Revised: 13 February 2025 Accepted: 25 February 2025 Published: 20 March 2025

Abstract

Background: The roles of small extracellular vesicles (sEVs) and mRNA modifications in regulating hepatitis B virus (HBV) transmission, replication, and related disease progression have received considerable attention. However, the mechanisms through which methyltransferase-like 3 (METTL3) and insulin-like growth factor 2 (IGF2BP2), key genes that mediate m6A modifications, regulate HBV replication in sEVs remain poorly understood. Therefore, this study investigated the molecular mechanisms through which the key molecules (METTL3 and IGF2BP2) in sEVs mediate m6A epigenetic modification to regulate HBV replication. Methods: Small extracellular vesicles were extracted from the supernatants of HepG2.2.15 and HepG2 cells via ultracentrifugation, followed by purification with hepatitis B virus surface antigen (HepBsAg) immunomagnetic beads. The sEVs were characterized by transmission electron microscopy (TEM), dynamic light scattering (DLS), and Western blotting (WB). Methylation enrichment in the two types of sEVs was analyzed by dot blotting and quantitative reverse transcription-PCR (RT-qPCR). The cells were treated with HepG2.2.15-sEVs transfected with either the METTL3 plasmid, METTL3 siRNA, the IGF2BP2 plasmid, or the IGF2BP2 siRNA. After 48 h, the expression of METTL3, IGF2BP2, and HBV DNA expressions were assessed via dot blotting, quantitative-PCR (qPCR), RT-qPCR, and WB. Coimmunoprecipitation (co-IP) was performed to investigate the interactions between METTL3 and IGF2BP2. Results: By conducting TEM, DLS, and WB analyses, we confirmed that the isolated sEVs exhibited typical characteristics. HepG2.2.15-derived sEVs presented elevated levels of m6A modifications, with increased METTL3 and IGF2BP2 mRNA and protein expression levels, respectively (p < 0.05). In the overexpression (OE)-METTL3 group, the expression levels of HBV pregenomic RNA (HBV pgRNA), HBV DNA, HBV relaxed circular DNA (HBV rcDNA), HBV covalently closed circular DNA (HBV cccDNA), HBsAg, hepatitis B virus core antigen (HBcAg), and hepatitis B virus e antigen (HBeAg) were significantly elevated compared to those in the control group (p < 0.01). In contrast, results for the small interfering (SI)-METTL3 group were the opposite. Similarly, in the OE-IGF2BP2 group, HBV pgRNA, HBV DNA, HBV rcDNA, HBV cccDNA, HBsAg, HBcAg, and HBeAg expression were greater than in the control group (p < 0.05), whereas the opposite results were recorded in the SI-IGF2BP2 group. Co-immunoprecipitation confirmed that METTL3 and IGF2BP2 interact synergistically. Conclusion: Small extracellular vesicles increase METTL3 and IGF2BP2 expression, synergistically promoting HBV replication by regulating m6A modification levels.

Keywords: HBV; small extracellular vesicles; N6-methyladenosine modification; METTL3; IGF2BP2

1. Introduction

Hepatitis B virus (HBV) possesses a 3.2 kb partial double-stranded relaxed circular DNA (*rcDNA*) genome, which can be repaired in the nucleus to covalently closed circular DNA (*cccDNA*) [1–3]. The *cccDNA* can be transcribed to generate new pregenomic RNA (*pgRNA*), which can produce new *rcDNA* via reverse transcription. This *rcDNA* can be secreted into the extracellular environment via small extracellular vesicles (sEVs), thus facilitating the infection of additional hepatocytes [4–6]. The primary factors contributing to persistent HBV infection include the chromosomal integration of *cccDNA* into host cells and infection mediated by sEVs [7]. However, the precise regulatory mechanisms underlying these processes remain poorly understood.

Small extracellular vesicles (sEVs) are bilayer vesicle structures characterized by a cup-shaped morphology, with particle sizes between 30 and 200 nm [8,9]. They are crucial in facilitating the transmission of HBV, disease progression, and the development of targeted therapy [10–12]. The study has indicated that interfering with extracellular vesicles significantly reduces HBV replication [13]. Moreover, engineered sEVs containing clustered regularly interspaced short palindromic repeats (Cas9/gR) and vesicular stomatitis virus-glycoprotein (VSV-G) can decrease HBV replication and *cccDNA* levels [14]. These findings highlight the close association between sEVs and the loading and dissemination of HBV viral particles, as sEVs contain various components, including *HBV DNA*, *HBV RNA*, and proteins [15,16].

¹Institute of Basic Medicine, North Sichuan Medical College, 637000 Nanchong, Sichuan, China

²Department of Laboratory Medicine, Xichong County People's Hospital, 637000 Nanchong, Sichuan, China

^{*}Correspondence: panwl@aliyun.com (Wanlong Pan)

Studies have shown that the m6A sites in the hepatitis C virus (HCV) can regulate the maturation of the virus in complex and undetermined ways [17,18]. Some researchers found that N6-methyladenosine binding protein (YTHDC2) mediates m6A modifications to regulate HCV internal ribosome entry site (IRES)-dependent translation [19]. The conserved m6A motifs located in the ϵ stemloop structures at the 3' end of the HBV mRNA and the 5' and 3' ends of the pgRNA represent critical sites for m6A modification [20]. Additionally, m6A modification increases pgRNA reverse transcription and increases HBV viral DNA levels, suggesting a significant role for m6A in the epigenetic regulation of HBV replication [1]. Methylation of the N6 position of adenine (m6A) is a prevalent posttranscriptional modification that influences biological processes by regulating the rates of splicing, translation, and decay of mRNAs [21-24]. M6A methylation is a dynamic and reversible epigenetic modification that is orchestrated by "readers", "writers", and "erasers" [25,26], and affects viral gene expression by recruiting various m6A-binding proteins throughout the life cycle of HBV [25]. These proteins play crucial roles in viral replication, the immune response, and oncogenesis [27].

Study has found that the proteins methyltransferase-like 3 (METTL3) and insulin-like growth factor 2 (IGF2BP2) that act as a writer and a reader, respectively, function as coregulators of m6A modification during HBV infection, with *METTL3* facilitating m6A enrichment in an *IGF2BP2*-dependent manner [28]. However, the precise mechanism by which sEVs mediate m6A epigenetic modifications to regulate HBV replication during viral packaging into sEVs for transmission to uninfected cells remains to be elucidated.

In our previous study, we found that METTL3 synergizes with IGF2BP2 to regulate HBV replication at the cellular level [29]. To further elucidate the specific molecular mechanisms through which sEVs mediate m6A modification and promote HBV replication via METTL3-IGF2BP2 synergy, we conducted this study. Unlike previous studies that focused on the cellular level, we regulated m6A modifications at the microscopic level in sEVs. We hypothesized that sEVs enhance HBV replication by modulating m6A levels through interactions between METTL3 and IGF2BP2. We examined changes in HBV replication markers by overexpressing or knocking down key m6A regulatory proteins, specifically the "writer" methyltransferase METTL3 and the "reader" protein IGF2BP2, in sEVs. We also characterized the mode of action of these proteins via co-immunoprecipitation (co-IP) to elucidate the mechanism by which sEVs mediate m6A modification to regulate HBV replication. We aimed to provide a framework to comprehensively elucidate the mechanisms underlying HBV replication and contribute to the discovery of novel molecular targets for treating HBV infection.

2. Materials and Methods

2.1 Cell Culture

HepG2.2.15 cells (iCell-h093, Shanghai ICell Bioscience Inc., Ltd., Shanghai, China) stably replicating HBV and their parental HepG2 cells (iCell-h092, Shanghai ICell Bioscience Inc., Ltd., Shanghai, China) were cultured in a medium consisting of 8% exosome-free fetal bovine serum (FBS) (Cat #EXO-FBS-50A-1, SBI, Palo Alto, CA, USA) supplemented with 1% penicillin streptomycin (Cat. NO. 15140122, Lot. 238344, Grand Island, NY, USA). To ensure stable HBV replication, HepG2.2.15 medium was supplemented with G418 solution at a concentration of 400 μg/mL (R20001, Lot.NO71R19494A, Shanghai Yuanye Bio-Technology Co., Ltd., Shanghai, China). All cell lines were validated via short tandem repeat (STR) profiling, were tested, and were found to be negative for mycoplasma (Supplementary materials).

2.2 Extraction of sEVs

After culturing HepG2 and HepG2.2.15 cells for 48–72 h, to remove impurities such as cells, the cell supernatants were collected and centrifuged at 3000 ×g for 30 min. Next, the small molecules were separated by centrifugation at 12,000 ×g for 45 min; subsequently, the supernatant was filtered through a 0.22 μm filter (REF.SLGPR33RE, Lot.R1DB07580, Merck Millipore, Billerica, MA, USA). Following this, sEVs were isolated via ultracentrifugation (MFG.NO. O11284, Hitachi himac-CP80NX, Tokyo, Japan) at 100,000 ×g for 120 min. The precipitated sEVs were resuspended in 1 mL of precooled 1×PBS (Cat. NO. P1022, Solarbio Science & Technology Co., Ltd., Beijing, China).

2.3 Purification of sEVs

Initially, 50 μ L of HepBsAg (S38: sc-52412, Santa Cruz Biotechnology, Santa Cruz, CA, USA) was added to the sEVs following ultracentrifugation. Then, they were transferred to a shaker and placed at 4 °C for 12 h to facilitate thorough rotation and mixing. Next, 20 μ L of Protein A/G PLUS-Agarose (sc-22003, Santa Cruz Biotechnology, Santa Cruz, CA, USA) was added, and the sample was incubated for 8 h at 4 °C with continuous mixing. After incubation, the mixture was centrifuged at $3000 \times g$ for 5 min to collect the supernatant, followed by ultracentrifugation at $100,000 \times g$ for 120 min. Finally, 100μ L of precooled $1 \times PBS$ was added to dissolve the pellet, resulting in the purification of sEVs with the removal of HBV virus particles.

2.4 Transmission Electron Microscope (TEM)

Purified sEVs from HepG2.2.15 cell culture supernatant (HepG2.2.15-sEVs) and HepG2 cell culture supernatant (HepG2-sEVs) were deposited onto a carbon-coated copper mesh, with $10~\mu L$ of each sample added to the grid.



After the excess liquid was aspirated from the edges, the samples were dried for 5 min. Next, 10 μL of 2% phosphotungstic acid (Cat# G1870, Lot No. 2400001, Beijing Solarbio Science & Technology Co., Ltd., Beijing, China) was added, and the mixture was stained for 1 min. Excess staining solution was removed, and the samples were dried overnight at room temperature. The morphology of the sEVs was observed and photographed using a transmission electron microscope (Hitachi HT7700, Tokyo, Japan).

2.5 Dynamic Light Scattering (DLS)

A 10 μ L sample of ultraisolated purified sEVs was added to 1 mL of 1 \times PBS, which was filtered through a 0.22 μ m filter, and the contents were thoroughly mixed. A zeta particle size analyzer (Malvern Zetasizer ZS90, Malvern, Worcestershire, UK) was used to measure the concentration and size distribution of the sEVs. Next, the number of particles and their diameters were plotted using Origin (Version Pro2021, 64-bit; Origin Lab Inc., Northampton, MA, USA).

2.6 Small Extracellular Vesicle Transfection

A 150 μ L transfection system for sEVs was prepared using the Exo-FectTM Exosome Transfection Reagent Kit (Cat#EXFT20A-1, Lot.230616-001, SBI, Palo Alto, CA, USA) as follows: 10 μ L of Exo-Fect, 20 μ L of nucleic acids (20 pmol siRNA or 5 μ g plasmid DNA), 50 μ L of purified HepG2.2.15-sEVs, and 70 μ L of sterile 1× PBS. The components were mixed by gently inverting the EP tubes six times without vortexing. The prepared mixture was placed in a shaker at 37 °C for 10 min and then transferred to ice. Next, 30 μ L of Exo Quick-TC was added to the mixture, and the contents were mixed by inverting the EP tube six times without vortexing to halt the transfection reaction. The transfected sEVs were maintained on ice (or 4 °C) for 30–40 min.

The sample suspension was centrifuged at 14,000 rpm for 3 min, and the precipitates were retained. At least 300 μ L of sterile 1× PBS was added to the precipitate, which was subsequently resuspended. The sequence of small interfering METTL3 (si-*METTL3*) was 5'-CCUGCAAGUAUGUUCACUATT-3', and that of small interfering IGF2BP2 (si-*IGF2BP2*) was 5'-GCATATACAACCCGGAAAGAA-3' (Cat.NO. M01, Guangzhou RiboBio Co., Ltd., Guangzhou, China).

Stably grown HepG2 cells were selected and seeded in six-well plates at a density of 2×10^5 cells/mL. Transfection was performed when the cells reached 60–80% confluence, about 12 h after seeding. Before transfection, the serum-free medium was removed. The mixture was subsequently incubated for 1 h with serum-free DMEM. Next, at least 150 μL of transfected HepG2.2.15-sEVs (containing siRNA or plasmid as described above) was added to the cells. After 4–6 h, the mixed medium was changed to nonresistant DMEM containing 8% exosome-free FBS.

The cells were allowed to grow for 48 h before being collected for subsequent experiments.

2.7 Quantitative Reverse Transcription-PCR (RT-qPCR)

Initially, RNA was extracted using the TRIzol (REF.15596026, Lot.257408, Thermo Fisher Scientific, Waltham, MA, USA) method. After determining its concentration, the RNA was reverse-transcribed to template cDNA in two steps using an RNA reverse transcription kit (REF.1622, Lot.3059833, Thermo Fisher Scientific, Waltham, MA, USA). In step 1, 1 μg of RNA and 1 μL of random primer were added, followed by the addition of ddH₂O to obtain a mixture of 12 μL. The prepared system was reacted at 65 °C for 5 min. In step 2, 4 μ L of 5× buffer, 2 μL of 10 mM dNTPs, 1 μL of RNase inhibitor, and 1 μL of reverse transcriptase were added sequentially. The reaction proceeded at 25 °C for 5 min, 42 °C for 60 min, and 70 °C for 5 min. The resulting cDNA served as a template for quantitative-PCR (qPCR) amplification using a fluorescent quantitative PCR detection kit (Cat.NO. CW0957, Beijing ComWin Biotech Co., Ltd., Beijing, China). Target gene expression was calculated using the $2^{-\Delta\Delta CT}$ method. All mRNA sequences of primers used were as follows [30-32] (Sangon Biotech Shanghai Co., Ltd., Shanghai, China): β-ACTIN F: 5'-CTCCATCCTGGCCTCGCTGT-3′, 5'-GCTGTCACCTTCACCGTTCC-3'; R: 5'-TTGTCTCCAACCTTCCGTAGT-**METTL3** F: 5'-CCAGATCAGAGAGGTGGTGTAG-3'; 3′, R: IGF2BP2 F: 5'-AGCTAAGCGGGCATCAGTTTG-3′, R: 5'-CCGCAGCGGGAAATCAATCT-3'; pgRNA 5'-CTCAATCTCGGGAATCTCAATGT-3′, R: 5'-TGGATAAAACCTAGGAGGCATAAT-3'; hepatitis B virus surface antigen 5'-TCACAATACCGCAGAGTC-3', R: ACATCCAGCGATAACCAG-3'; hepatitis B virus core antigen (HBcAg) F: 5'-CTGGGTGGGTGTTAATTTGG-3', 5'-TAAGCTGGAGGAGTGCGAAT-3′; hepatitis B virus e antigen (HBeAg)F: 5'-5'-GATTCGCACTCCTCCAGTCT-3', AGTTCTTCTTCTAGGGGACCTG-3'.

2.8 m6A Dot Blotting

After extracting RNA using the TRIzol method and determining its concentration, the RNA samples were serially diluted to 200 ng/ μ L, 100 ng/ μ L, and 50 ng/ μ L. The samples were subsequently denatured in a metal bath at 95 °C for 5 min and then cooled immediately on ice. Next, 2 μ L of each RNA sample was added dropwise onto a nylon (NC) membrane, which had been cut to the appropriate size. After the RNA was allowed to diffuse naturally and dry, the membrane was cross-linked under UV light for 2 h. Following the cross-linking step, the sealing solution was closed for 1 h.

The NC membrane was incubated at 4 °C for 12–16 h with the primary m6A antibody (dilution 1:1000, Cat. NO.



517924, Lot. NO. KK0512, Chengdu ZEN-BIOSCIENCE Co., Ltd., Chengdu, China). The HRP-labeled goat antirabbit IgG secondary antibody (1:5000, Cat.NO. FNSA-0004, Chengdu ZEN-BIOSCIENCE Co., Ltd., Chengdu, China) was added, and the mixture was shaken gently at room temperature for 1 h. The signal was developed using an ECL detection system after washing the film.

2.9 HBV DNA Extraction and Characterization

An animal tissue/cellular genomic DNA extraction kit was used to extract cellular *HBV DNA* (Cat# D1700, Lot No. 2311002, Solarbio Science & Technology Co., Ltd., Beijing China), and its concentration was subsequently determined. To digest the *HBV DNA*, the sample was incubated with T5 nucleic acid exonuclease (D7082S-1, Shanghai Biyuntian Biotechnology Co., Ltd., Shanghai, China) for 30 min at 37 °C. The samples were terminated by adding EDTA and then heat-inactivated at 95 °C for 5 min.

PCR amplification was first performed using primers for *HBV DNA*, *HBV rcDNA*, and *HBV cccDNA*, and then the copy number of the DNA was calculated based on a standard curve. The sequences of primers used were as follows (Sangon Biotech Shanghai Co., Ltd., Shanghai, China): *HBV DNA* F: 5'-ACCGACCTTGAGGCATACTT-3', R: 5'-GCCTACAGCCTCCTAGTACA-3'; *HBV rcDNA* F: 5'-TTTCACCTCTGCCTAATCATCTCT-3', R: 5'-CTTTATAAGGGTCGATGCCATGC-3'; and *HBV cc-cDNA* F: 5'-GCCTATTGATTGATTGGAAAGTATGT-3', R: 5'-AGCTGAGGCGGTATCTA-3'.

2.10 Western Blotting

The cells and sEVs were lysed in RIPA buffer containing 1% PMSF (ST507, Shanghai Biyuntian Biotechnology Co., Ltd., Shanghai, China) to extract total protein. The samples were lysed on ice for 30 min and centrifuged at $12,000 \times g$ for 30 min at 4 °C to collect the supernatant. The protein concentration was estimated by the BCA method. (Cat# PC0021, Solarbio Science & Technology Co., Ltd., Beijing, China).

After normalizing the protein concentrations, equal amounts of protein were separated by SDS-PAGE and transferred to 0.45 µm PVDF membranes. Next, 5% skim milk powder was added for 1 h, after which the appropriate primary antibody (METTL3, IGF2BP2 primary antibody dilution of 1:1000; Chengdu ZEN-BIOSCIENCE Co., Ltd., Chengdu, China) was added, and the membrane was incubated at 4 °C for 12-16 h. After washing three times with TBST, the membrane was incubated with an HRPconjugated secondary antibody (1:5000, Cat.NO. FNSA-0004, Chengdu ZEN-BIOSCIENCE Co. Ltd., Chengdu, China) at room temperature for 1 h. After the film was washed, the protein bands were detected using an ECL detection system. The ImageJ software (Version 1.54v, Java1.8.0, 64-bit; Media Cybernetics, Silver Springs, MD, USA) was used to analyze the Western blotting bands in

grayscale, and the results were normalized by dividing the target protein grayscale value by an internal reference grayscale value. The primary antibodies used were as follows: β-ACTIN (1:10,000, AC004, ABclonal Technology, Wuhan, China), Alix (1:1000, NO.2215, ABclonal Technology, Wuhan, China), CD63 (1:1000, A19023, ABclonal Technology, Wuhan, China), CD9 (1:1000, A19027, ABclonal Technology, Wuhan, China), GAPDH (R380646, 1:5000, Chengdu ZEN-BIOSCIENCE Co., Ltd., Chengdu, China), METTL3 (R508370, 1:1000, Chengdu ZEN-BIOSCIENCE Co., Wuhan, China), IGF2BP2 (R389232, 1:1000, Chengdu ZEN-BIOSCIENCE Co., Ltd., Chengdu, China).

2.11 Co-Immunoprecipitation

After the cells were transfected with sEVs containing the *METTL3* plasmid, they were harvested 48 h posttransfection to prepare protein samples. Following the protocol, 20 μL of protein A+G magnetic beads (Cat. NO. P2179S, Lot NO.091322230131, Shanghai Biyuntian Biotechnology Co., Ltd., Shanghai, China) were mixed with 2 μg of either *METTL3* primary antibody or normal rabbit IgG and incubated at room temperature for 4 h. Next, protein samples of equal mass were added, and the mixture was rotated overnight at 4 °C.

After incubation, the beads and supernatant were separated using a magnetic rack for 1 min. Next, 500 μL of a lysis buffer supplemented with protease inhibitors was used to wash the beads three times. After washing, 50 μL of $1\times$ SDS-PAGE protein loading buffer was added to the beads, and the mixture was heated at 95 °C for 10 min to elute the proteins. The supernatant was then collected after the magnetic beads were separated using a magnetic rack. Finally, the samples were analyzed by SDS-PAGE.

2.12 Statistical Analysis

All data were presented as the mean \pm standard deviation (SD) derived from three independent experiments. Data were analyzed and graphs were made using Graph-Pad Prism (version 10.1.2, GraphPad Software, Inc., CA, USA). An independent samples t-test was conducted for pairwise comparisons, and a one-way analysis of variance (ANOVA) followed by Šídák's multiple comparison test was conducted for multiple group comparisons. All differences among and between groups were considered to be statistically significant at p < 0.05.

3. Results

3.1 Identification of sEVs

Small extracellular vesicles derived from HepG2 cells (HepG2-sEVs) and HepG2.2.15 cells (HepG2.2.15-sEVs) were characterized following purification by ultracentrifugation. DLS analysis revealed that 82.4% of the HepG2-sEV particles were 30–200 nm in size, and the peak particle size and concentration were 122.4 nm and 2.30 ×



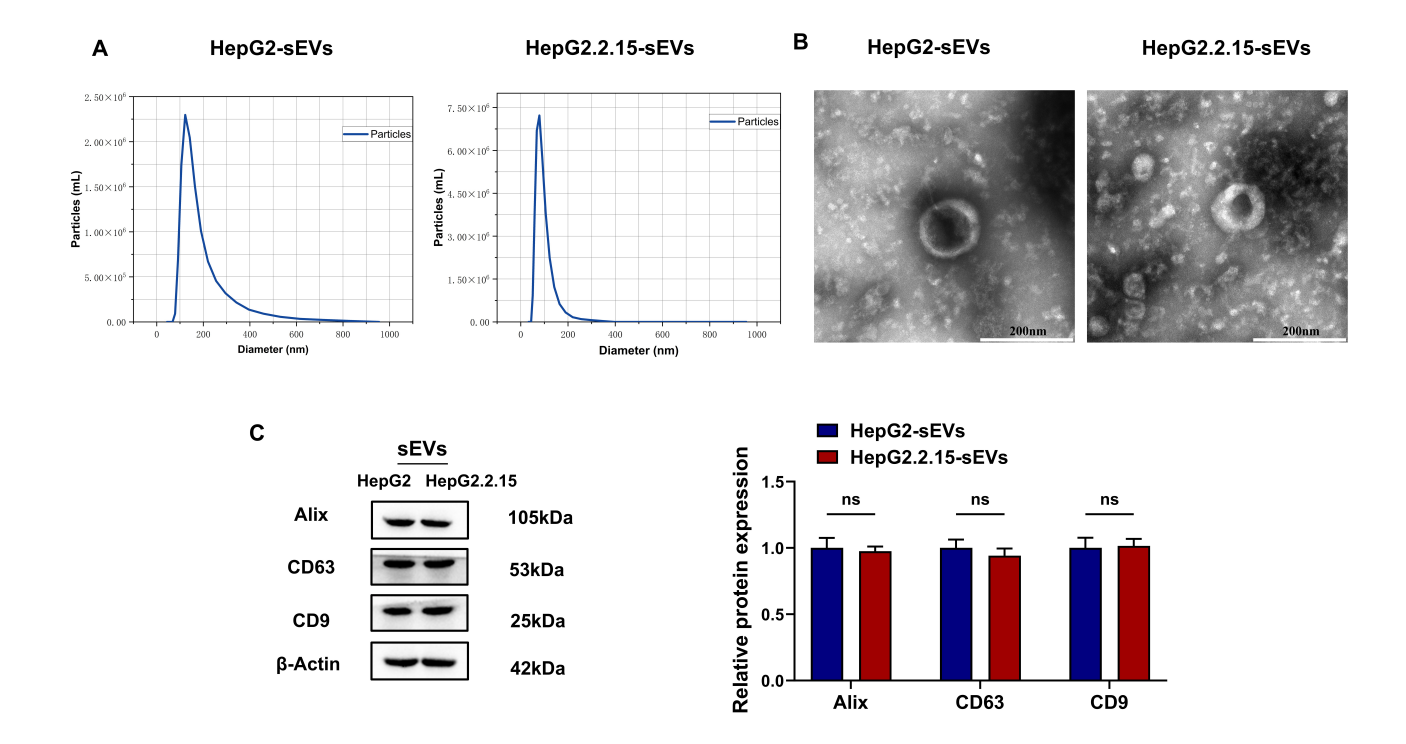


Fig. 1. Identification of sEVs following ultracentrifugation purification. (A) DLS analysis was conducted to measure the size of sEVs. (B) TEM imaging was performed to investigate the morphological structure of sEVs. The scale bar = 200 nm. (C) Western blotting analysis was performed to detect marker proteins associated with sEVs; ns p > 0.05. sEVs, small extracellular vesicles; DLS, dynamic light scattering; TEM, transmission electron microscopy.

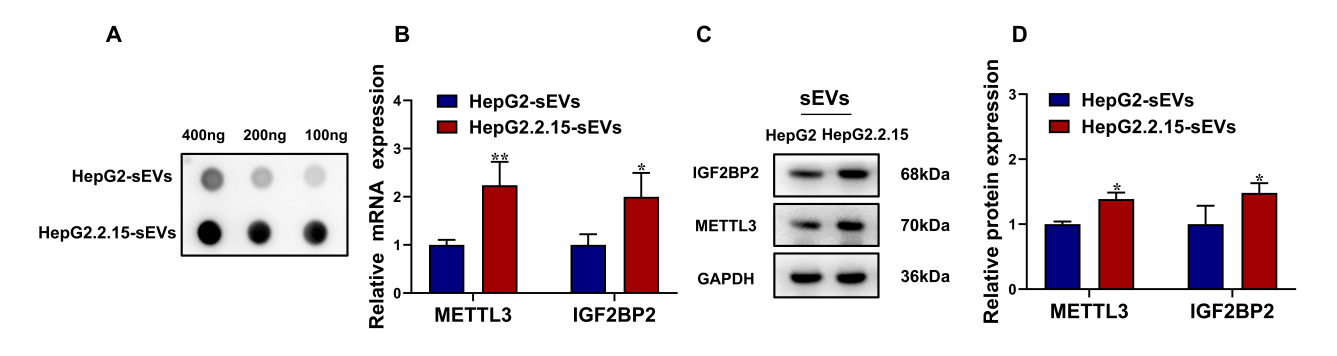


Fig. 2. Enrichment of m6A methylations in sEVs isolated from the HBV-stably replicating HepG2.2.15 cell line. (A) Dot blotting was performed to detect the m6A modification levels in the two kinds of sEVs. (B) Quantitative reverse transcription-PCR (RT-qPCR) was performed to measure the mRNA expression levels of the methyltransferase METTL3 and the reader protein IGF2BP2 in both types of sEVs. (C,D) Western blotting was conducted to assess the protein expression levels of METTL3 and IGF2BP2; *p < 0.05 and **p < 0.01. HBV, hepatitis B virus; METTL3, methyltransferase-like 3; IGF2BP2, insulin-like growth factor 2.

 10^6 particles/mL, respectively. In contrast, 98.7% of the HepG2.2.15-sEV particles were also 30–200 nm in size and exhibited peak sizes and concentrations of 78.82 nm and 7.22×10^6 particles/mL, respectively (Fig. 1A). TEM demonstrated that both types of sEVs had a double-layered membranous structure with an average diameter of about 100 nm (Fig. 1B). Additionally, the WB analysis confirmed that the characteristic sEV proteins, including Alix, CD63, and CD9, were expressed (Fig. 1C).

3.2 Enrichment of m6A Methylation in sEVs Derived From the HBV Stably Replicating the HepG2.2.15 Cell Line

Compared to HepG2-sEVs, HepG2.2.15-sEVs presented significantly greater levels of m6A methylation (Fig. 2A). The expression levels of *METTL3* and *IGF2BP2* mRNAs in HepG2.2.15-sEVs were significantly elevated, as determined by RT-qPCR analysis (Fig. 2B; p < 0.05). The results of the Western blotting analysis revealed a corresponding increase in protein levels (Fig. 2C,D; p < 0.05).



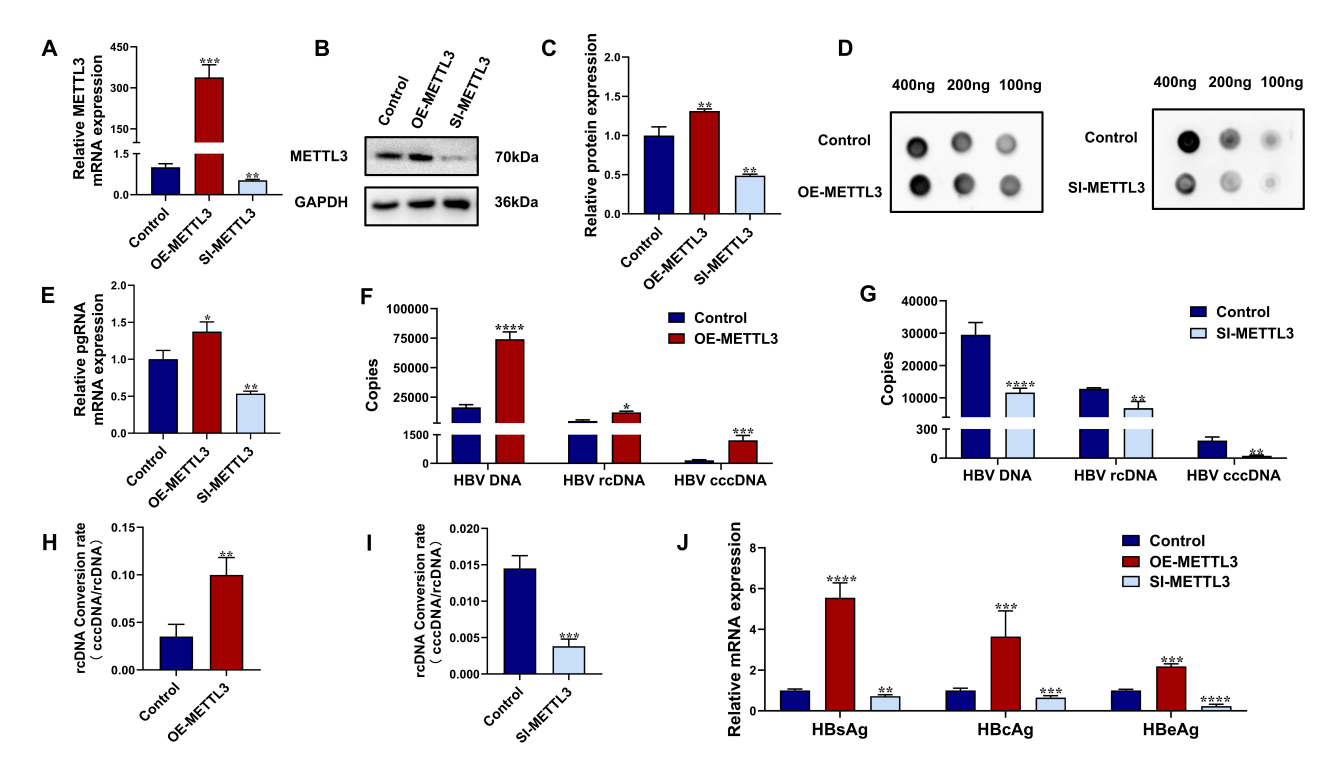


Fig. 3. HepG2.2.15-sEVs enhance HBV replication by upregulating the methyltransferase METTL3. In the control group, HepG2.2.15-sEVs without transfection were introduced into parental HepG2 cells. In the OE-METTL3 group, HepG2.2.15-sEVs overexpressing METTL3 were transfected into HepG2 cells after transfection with the METTL3 plasmid. In the SI-METTL3 group, HepG2.2.15-sEVs with METTL3 knockdown were transfected into HepG2 cells after transfection with METTL3 siRNA. (A) RT-qPCR was performed to detect the mRNA expression level of METTL3. (B,C) Western blotting analyses were performed to assess the METTL3 protein level. (D) Dot blot analyses were performed to evaluate the level of m6A modification. (E–J) qPCR and RT-qPCR analyses were performed to measure the expression rates of pgRNA, HBV DNA, HBV rcDNA, and HBV rcDNA, the rcDNA conversion rate, and the mRNA expression levels of HBsAg, HBcAg, and HBeAg; *p < 0.05, **p < 0.01, ***p < 0.001, and ****p < 0.0001. pgRNA, pregenomic RNA; rcDNA, relaxed circular DNA; rcDNA, covalently closed circular DNA; methyltransferase-like 3; OE, overexpression; SI, small interfering RNA; methyltransferase-like 3; OE, o

These findings suggested that an increase in m6A methylation levels in HepG2.2.15-sEVs is associated with the replication of HBV.

3.3 HepG2.2.15-sEVs Promote HBV Replication Through Upregulation of the Methyltransferase METTL3

METTL3 was overexpressed or knocked down in HepG2.2.15-sEVs, resulting in corresponding alterations in *METTL3*. In the overexpressing METTL3 (OE-METTL3) group, the *METTL3* mRNA and protein levels increased. Conversely, in the SI-METTL3 group, *METTL3* mRNA and protein levels were lower than those in the control group (Fig. 3A–C; p < 0.01), confirming that *METTL3* expression was modulated. Moreover, the levels of m6A modification exhibited a corresponding increase or decrease (Fig. 3D).

Compared to that in parental HepG2 control cells treated with untransfected HepG2.2.15-sEVs, the mRNA level of *HBV pgRNA*, a marker of HBV replication, was significantly greater in the OE-METTL3 group (Fig. 3E; *p*

< 0.05). The *HBV DNA*, *HBV rcDNA*, and *HBV cccDNA* copy numbers also increased significantly (Fig. 3F; p < 0.05), whereas the *HBV rcDNA* conversion rate increased from 3.51% to 9.99% (Fig. 3H; p < 0.01). Moreover, the *HBsAg*, *HBcAg*, and *HBeAg* mRNA expression levels increased (Fig. 3J; p < 0.001).

In contrast, the SI-METTL3 group presented a decrease in viral replication indicators: $HBV\ pgRNA$ expression decreased (Fig. 3E; p < 0.01), and the copy numbers of $HBV\ DNA$, $HBV\ rcDNA$, and $HBV\ cccDNA$ decreased (Fig. 3G; p < 0.01). The $HBV\ rcDNA$ conversion rate decreased from 1.45% to 0.38% (Fig. 3I; p < 0.001), and the mRNA levels of HBsAg, HBcAg, and HBeAg decreased (Fig. 3J; p < 0.01).

These results suggested that HepG2.2.15-sEVs facilitated an increase in m6A methylation through the upregulation of *METTL3*, which promoted the conversion of *rcDNA* to *cccDNA*, thereby regulating the replication of HBV. Inhibition of *METTL3* expression decreased *HBV DNA* levels in



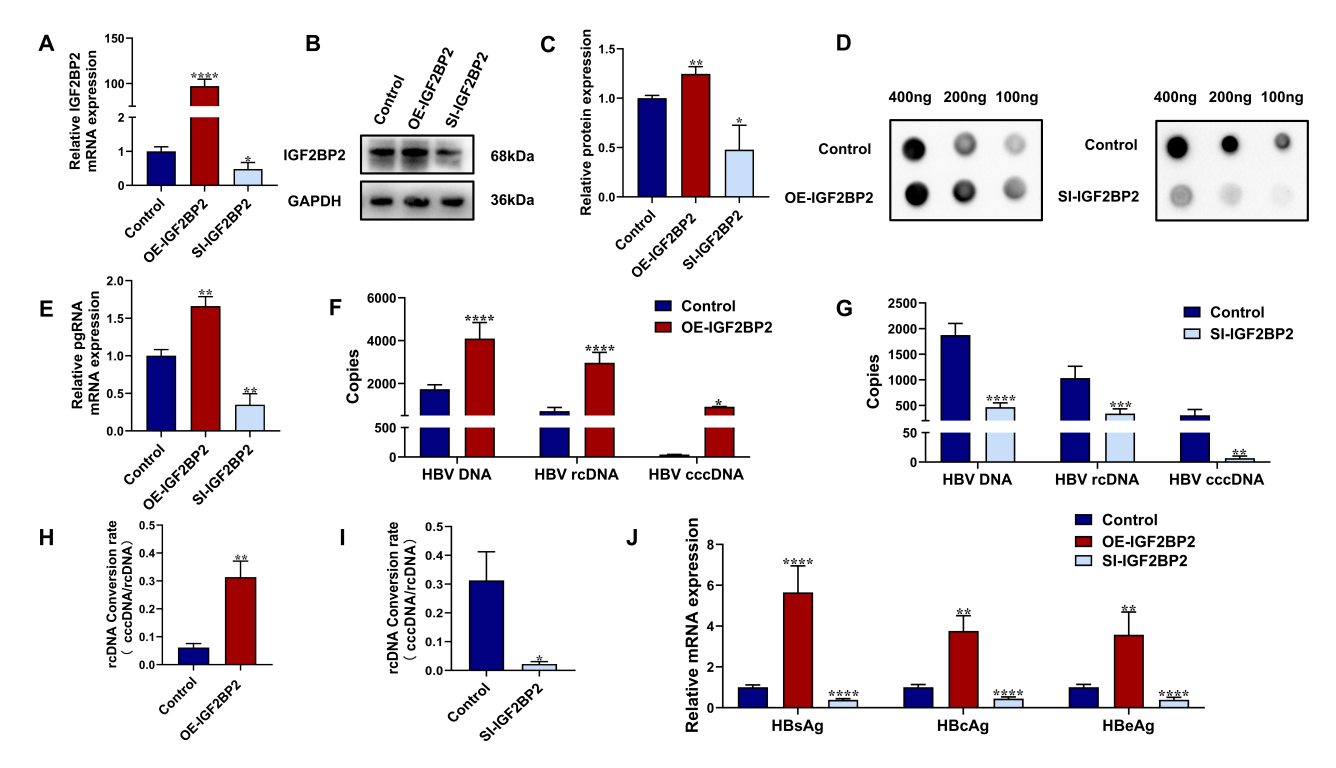


Fig. 4. HepG2.2.15-sEVs enhance HBV replication through IGF2BP2. In the control group, untransfected HepG2.2.15-sEVs were introduced into HepG2 cells. In the OE-IGF2BP2 group, HepG2.2.15-sEVs were transfected into HepG2 cells following transfection with an IGF2BP2 plasmid to induce the overexpression of IGF2BP2. In the SI-IGF2BP2 group, HepG2.2.15-sEVs were transfected into HepG2 cells after transfection with IGF2BP2 siRNA to knock down IGF2BP2. (A) The overexpression or knockdown of IGF2BP2 was confirmed by RT-qPCR to measure IGF2BP2 mRNA expression. (B,C) The overexpression or knockdown of IGF2BP2 was confirmed by Western blotting analysis to assess the level of the IGF2BP2 protein. (D) The level of m6A modification resulting from the overexpression or knockdown of IGF2BP2 was evaluated by dot blot analysis. (E–J) The effect of knocking down or overexpressing IGF2BP2 on HBV replication was assessed through RT-qPCR and qPCR; the expression levels of pgRNA, HBV DNA, HBV rcDNA, and HBV rcDNA; the rcDNA conversion rates; and the mRNA levels of HBsAg, HBcAg, and HBeAg were measured; *p < 0.05, **p < 0.01, ***p < 0.001, and ****p < 0.0001. IGF2BP2, insulin-like growth factor 2.

the treatment of HBV-associated diseases, and the detection of *METTL3* in sEVs may be used to predict HBV-associated diseases and monitor the prognosis of the disease caused by HBV.

3.4 HepG2.2.15-sEVs Promote HBV Replication Through the Reader Protein IGF2BP2

The IGF2BP2 mRNA expression levels increased or decreased (Fig. 4A; p < 0.05) following the overexpression or knockdown of IGF2BP2 in HepG2.2.15-sEVs, as determined by RT-qPCR analysis. The results of the Western blotting assays demonstrated an increase or decrease in the IGF2BP2 protein expression level (Fig. 4B,C; p < 0.05), confirming that IGF2BP2 was successfully manipulated in sEVs. Concurrently, the level of m6A modification was also altered (Fig. 4D).

Compared to the parental HepG2 control cells treated with untransfected HepG2.2.15-sEVs, the expression level of HBV pgRNA, a marker for detecting HBV replication, increased or decreased (Fig. 4E; p < 0.01). The HBsAg,

HBcAg, and HBeAg mRNA levels increased or decreased, respectively (Fig. 4J; p < 0.01).

The copy numbers of *HBV DNA*, *HBV rcDNA*, and *HBV cccDNA* increased (Fig. 4F; p < 0.05), with the *HBV rcDNA* conversion rate increasing from 6.14% to 31.34% (Fig. 4H; p < 0.01). In contrast, these values decreased (Fig. 4G; p < 0.01), with the *HBV rcDNA* conversion rate decreasing from 31.25% to 2.23% (Fig. 4I; p < 0.05).

These results suggested that HepG2.2.15-sEVs, via the reader protein IGF2BP2, can increase m6A levels, promote the conversion of *rcDNA* to *cccDNA*, and consequently regulate the replication of HBV. A significant reason for the prolonged treatment of HBV disease is the difficulty in eliminating *cccDNA*. These experimental results suggested that the *rcDNA* conversion rate may be reduced by inhibiting the expression of *IGF2BP2*, thus decreasing the generation of *cccDNA* and halting the progression of the disease.



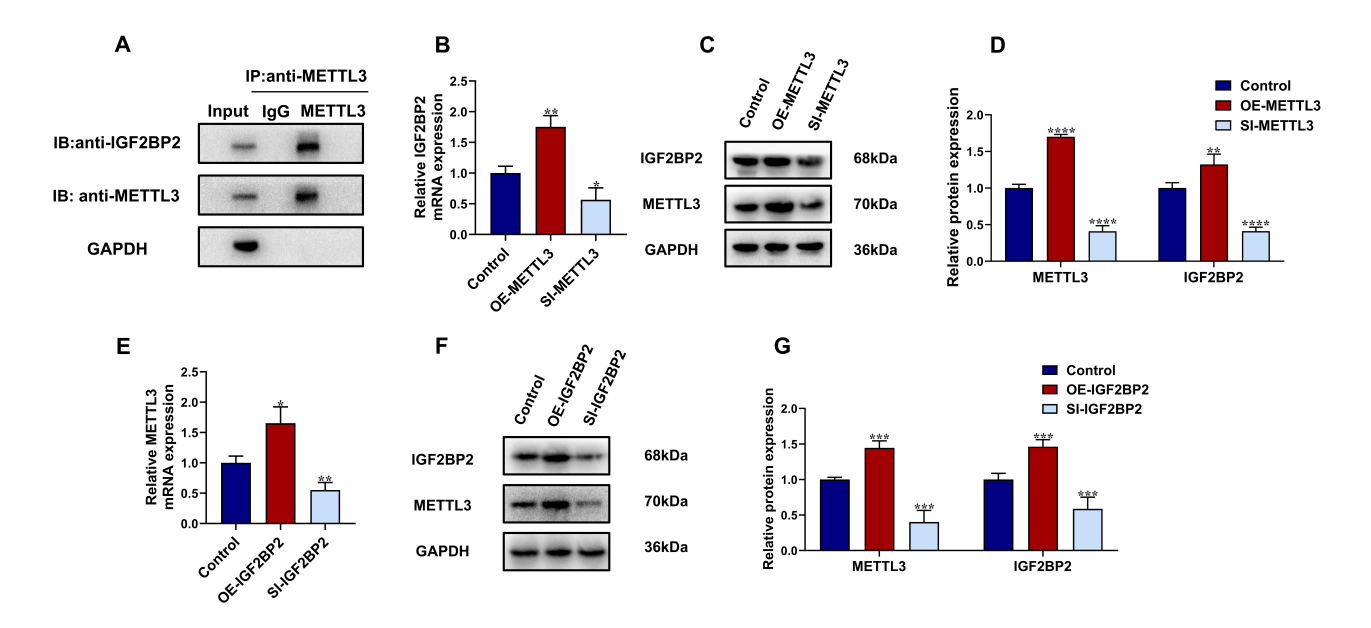


Fig. 5. METTL3 synergizes with IGF2BP2 in HepG2.2.15-sEVs. The control group consisted of HepG2.2.15-sEVs transfected into HepG2 cells. The OE-METTL3 group included HepG2.2.15-sEVs overexpressing METTL3, which were also transfected into HepG2 cells. In the SI-METTL3 group, HepG2.2.15-sEVs with METTL3 knockdown were transfected into HepG2 cells. The OE-IGF2BP2 group included HepG2.2.15-sEVs overexpressing IGF2BP2, which were transfected into HepG2 cells, whereas the SI-IGF2BP2 group included HepG2.2.15-sEVs with IGF2BP2 knockdown, which were also transfected into HepG2 cells. (A) Co-IP experiments were conducted to confirm the interaction between METTL3 and IGF2BP2. (B) Following the overexpression or knockdown of METTL3, RT-qPCR was performed to assess IGF2BP2 mRNA expression. (C,D) Western blotting analysis was performed to evaluate METTL3 and IGF2BP2 protein levels after the overexpression or knockdown of METTL3. (E) RT-qPCR analysis was performed to measure METTL3 mRNA levels following the overexpression or knockdown of IGF2BP2: *p < 0.05, **p < 0.01, ***p < 0.001, and ****p < 0.0001.

3.5 Methyltransferase METTL3 Synergizes With the Reader Protein IGF2BP2 in HepG2.2.15-sEVs

After the cells were transfected with HepG2.2.15-sEVs containing the *METTL3* plasmid, IGF2BP2 was detected via immunoprecipitation (IP) using an anti-*METTL3* antibody. The immunoprecipitation results indicated a synergistic interaction between METTL3 and IGF2BP2 (Fig. 5A).

After the cells were transfected with HepG2.2.15-sEVs with either overexpression or knockdown of *METTL3*, the *IGF2BP2* mRNA expression level increased, as determined by RT-qPCR (Fig. 5B; p < 0.01). The results of the Western blotting analysis revealed that the METTL3 and IGF2BP2 protein levels increased and decreased, respectively (Fig. 5C,D; p < 0.01).

After the cells were transfected with HepG2.2.15-sEVs with either overexpression or knockdown of IGF2BP2, the METTL3 mRNA expression levels increased or decreased, respectively (Fig. 5E; p < 0.05). Similarly, the METTL3 and IGF2BP2 protein levels increased or decreased, respectively (Fig. 5F,G; p < 0.001). These results confirmed the synergistic relationship between METTL3 and IGF2BP2.

4. Discussion

We previously reported that sEVs carry HBV components that evade immune surveillance, allowing the virus to spread to uninfected cells and promote the replication of HBV [33,34]. These sEVs possess a stable phospholipid bilayer structure that effectively prevents the degradation of HBV components, and their membrane composition closely resembles that of cellular membranes, facilitating efficient cellular uptake. Among the membrane markers of sEVs, *CD63* plays a key role in the packaging, transport, and release of nascent HBV [35]. These findings indicate the importance of sEVs as significant participants and signaling mediators in HBV infection [36,37].

METTL3-mediated and IGF2BP2-mediated m6A modifications have attracted considerable attention. One study showed that the METTL3-IGF2BP2 complex can promote inflammation through m6A modification, providing important information for the treatment of sepsis [38]. Another study revealed that METTL3 and IGF2BP2 influence the progression of colorectal cancer in a m6A modification-dependent manner [39]. Several studies support the notion that METTL3 and IGF2BP2-mediated m6A modifications play broad roles in various pathogenic



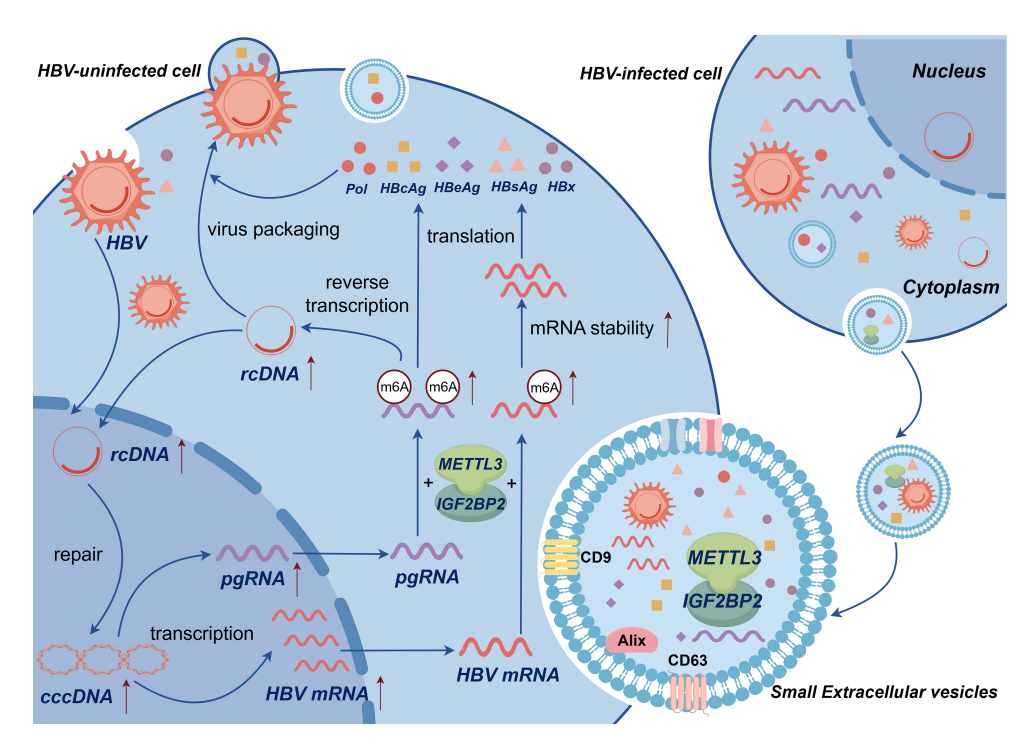


Fig. 6. Mechanistic model in which *METTL3* and *IGF2BP2* synergistically mediate m6A modification to regulate HBV replication. Small extracellular vesicles (sEVs) enhance m6A epigenetic modification through the coordinated action of *METTL3* and *IGF2BP2*. This process facilitates the conversion of *HBV rcDNA* to *cccDNA*, increases the level and stability of HBV core gene mRNA transcripts, including *pgRNA*, *HBsAg*, *HBcAg*, and *HBeAg*, and ultimately regulates the replication and transcription of HBV (Source: Figdraw 2.0, a platform from China affiliated with the House of Researchers).

mechanisms. Studies have also shown that m6A modifications in HBV RNA may affect its stability and translation, subsequently affecting viral replication [20,33,40]. However, the mechanisms by which sEVs mediate epigenetic modifications remain poorly understood. One study indicated that the expression of the methyltransferase *METTL3* was significantly higher in the liver tissues of patients with HBV-associated hepatocellular carcinoma compared to normal tissues [41]. This study also suggested that *METTL3*-mediated m6A modification is crucial for maintaining mRNA stability in an *IGF2BP2*-dependent manner [42].

Based on these findings, we hypothesized that sEVs mediate m6A epigenetic modifications to promote HBV replication through the *METTL3-IGF2BP2* pathway. Our results indicated that *METTL3* and *IGF2BP2* expression levels were higher in the HBV-stably replicating HepG2.2.15 cell line compared to their expression levels in HepG2 cells [29]. Additionally, m6A modification was significantly enriched in HepG2.2.15-sEVs, suggesting a close association between m6A modification in sEVs and HBV replication.

To elucidate the specific mechanism by which *METTL3* and *IGF2BP2* co-mediate m6A modification in sEVs to regulate HBV replication, the *METTL3* gene, a key enzyme, was either overexpressed or knocked down in HepG2.2.15-sEVs, which were subsequently used to trans-

fect HepG2 cells. The results indicated a corresponding increase or decrease in m6A methylation, along with alterations in HBV DNA copy number and HBV pgRNA expression. These findings suggested that METTL3 facilitates HBV DNA replication by increasing the m6A modification of HBV mRNAs in sEVs and increasing pgRNA expression levels. A probable mechanism may be as follows: METTL3 regulates HBV replication by targeting m6A modification sites located in the ε -stem-loop structure at the 3' end of the HBV mRNA and the 5' and 3' ends of pgRNA [20].

Transfection of HepG2 cells with HepG2.2.15-sEVs that either overexpress or knock down METTL3 resulted in a considerable increase or decrease in the mRNA levels of HBsAg, HBcAg, and HBeAg. These findings suggested that METTL3 within sEVs influences the transcription of HBV core proteins and cytosolic proteins, thus leading to an increase in mRNA expression levels. This regulation affects HBV viral packaging and promotes viral replication. A similar observation was reported in a related study by Cheng et al. [43]. Furthermore, an examination of the HBV viral genomic rcDNA and cccDNA revealed that the copy numbers of rcDNA and cccDNA changed simultaneously, accompanied by a significant alteration in the rcDNA to cccDNA conversion rate. These findings indicated that METTL3 in sEVs enhances HBV replication by increasing the expression of HBV rcDNA and cccDNA, as well as by



facilitating the conversion of *rcDNA* to *cccDNA*, which in turn supports the replication of HBV [1,2,44].

We found that sEVs-mediated *METTL3* enhances m6A methylation of *HBV mRNA* and *pgRNA*, resulting in an increase in the levels of *HBV DNA* and promoting the conversion of *rcDNA* to *cccDNA*. This process serves as a template that enhances the transcription of core viral proteins (*HBsAg*, *HBcAg*, and *HBeAg*), ultimately regulating the replication and transcription of HBV.

Further experiments involving the overexpression or knockdown of IGF2BP2 in sEVs revealed a significant increase or decrease in the copy number of HBV DNA, indicating that IGF2BP2 also plays a role in regulating HBV replication within sEVs. This finding aligned with observations at the cellular level that a targeted reduction in IGF2BP2 inhibits the proliferation of HepG2.215 cells and viral replication [45]. To elucidate the mechanism underlying the role of IGF2BP2 in sEVs, the copy numbers of rcDNA and cccDNA were also examined. The results indicated that overexpressing or knocking down IGF2BP2 in sEVs increased or decreased rcDNA and cccDNA copy numbers in transfected HepG2 cells, along with a corresponding increase or decrease in the rcDNA to cccDNA conversion rate. These findings suggested that IGF2BP2 enhances the expression of rcDNA and cccDNA and promotes the conversion of rcDNA to cccDNA, thereby facilitating the replication of HBV.

The overexpression or knockdown of IGF2BP2 in sEVs resulted in an increase or decrease in the mRNA expression levels of pgRNA, HBsAg, HBcAg, and HBeAg, respectively, along with corresponding alterations in m6A methylation levels in transfected HepG2 cells. These findings indicated that IGF2BP2 in sEVs mediates m6A modifications to positively regulate the transcription of HBV RNA. IGF2BPs can recognize GGm6AC motifs, thus promoting mRNA translation and enhancing mRNA stability [46–48]. Based on these findings, we speculated that IGF2BP2 in sEVs binds to HBV mRNA, enhancing its stability and promoting translation. This interaction increases mRNA expression of HBV core proteins and cytosolic proteins and also elevates viral DNA levels. This process also facilitates the conversion of rcDNA to cccDNA, thereby regulating the replication and transcription of HBV. Although functionally similar to METTL3, the underlying mechanisms probably differ.

Therefore, the mechanism of action of *METTL3* and *IGF2BP2* is critical. After *METTL3* and *IGF2BP2* in sEVs were overexpressed or knocked down, we found a corresponding increase or decrease in the expression levels of *IGF2BP2* and *METTL3* in the transfected cells. Co-IP experiments showed a synergistic interaction between *METTL3* and *IGF2BP2*. These findings suggested that sEVs regulate HBV replication through the collaborative interaction of *METTL3* and *IGF2BP2*, which mediates m6A methylation. Some studies have also shown that

the *METTL3-IGF2BP2* axis can interact to regulate m6A methylation [21,49,50]. The methyltransferase *METTL3* and the reading protein *IGF2BP2* work synergistically to form a complex; the process involved is intricate and involves multiple molecules. Among these molecules, the most notable players include *IGF2BP1* and *IGF2BP3* from the *IGF2BP* family, which frequently bind to *IGF2BP2* [21]. Therefore, we hypothesized that they may also play a role in the synergistic action of *METTL3* and *IGF2BP2*. However, this hypothesis needs to be experimentally verified.

In this study, we investigated the mechanisms regulating HBV replication, beginning at the molecular level of sEVs, while integrating the contemporary research interest in m6A methylation (Fig. 6). This approach offers a relatively novel perspective; however, other genetic components and regulatory pathways may also be involved. For example, *IGF2BP2* can directly bind to the structure-specific nuclease Flap Structure-Specific Endonuclease 1 (*FEN-1*) mRNA, thereby influencing the stability of *FEN-1*, which presents an additional avenue for future research. However, our study had some limitations, including the absence of certain *in vivo* experimental data. Therefore, further investigations are needed, and we aim to assess these avenues in our future study.

5. Conclusion

To summarize, sEVs enhance m6A epigenetic modification through the synergistic interaction of *METTL3* and *IGF2BP2*, promoting the conversion of *HBV rcDNA* to *cc-cDNA* and increasing the mRNA transcript levels of *HBV* core genes, including *pgRNA*, *HBsAg*, *HBcAg*, and *HBeAg*. This process regulates HBV replication and transcription. In this study, we investigated the molecular mechanism by which *METTL3* and *IGF2BP2* collaborate to mediate m6A methylation in sEVs, thereby regulating the replication of HBV. However, the effect of sEVs and their contents on HBV regulation necessitates further validation through additional studies. These findings may serve as a basis for developing new therapeutic targets and pathways for treating HBV infection.

Availability of Data and Materials

The datasets used during the current study are available from the corresponding author on reasonable request.

Author Contributions

JZ and WP designed the research study, JZ performed the research and analyzed the data, LY and XW gave guidance on experimental techniques. All authors contributed to editorial changes in the manuscript. All authors read and approved the final manuscript. All authors have participated sufficiently in the work and agreed to be accountable for all aspects of the work.



Ethics Approval and Consent to Participate

Not applicable.

Acknowledgment

We thank Sichuan North Medical College for providing the platform to complete the experiments and Nanchong Municipal Science and Technology Strategic Cooperation Program with Colleges and Universities for the financial support.

Funding

The work was supported by the Special Project of Strategic Cooperation in Science and Technology of Nanchong City and Colleges and Universities (22SXQT0318).

Conflict of Interest

The authors declare no conflict of interest.

Supplementary Material

Supplementary materials associated with this article can be found, in the online version, at https://doi.org/10.31083/FBL36291.

References

- [1] Kostyusheva A, Brezgin S, Glebe D, Kostyushev D, Chulanov V. Host-cell interactions in HBV infection and pathogenesis: the emerging role of m6A modification. Emerging Microbes & Infections. 2021; 10: 2264–2275. https://doi.org/10.1080/22221751.2021.2006580.
- [2] Wei L, Ploss A. Mechanism of Hepatitis B Virus cccDNA Formation. Viruses. 2021; 13: 1463. https://doi.org/10.3390/ v13081463.
- [3] Allweiss L, Testoni B, Yu M, Lucifora J, Ko C, Qu B, et al. Quantification of the hepatitis B virus cccDNA: evidence-based guidelines for monitoring the key obstacle of HBV cure. Gut. 2023; 72: 972–983. https://doi.org/10.1136/gutjnl-2022-328380.
- [4] Bhat SA, Kazim SN. HBV cccDNA-A Culprit and Stumbling Block for the Hepatitis B Virus Infection: Its Presence in Hepatocytes Perplexed the Possible Mission for a Functional Cure. ACS Omega. 2022; 7: 24066–24081. https://doi.org/10.1021/ac somega.2c02216.
- [5] Wei L, Ploss A. Hepatitis B virus cccDNA is formed through distinct repair processes of each strand. Nature Communications. 2021; 12: 1591. https://doi.org/10.1038/s41467-021-21850-9.
- [6] Ko C, Chakraborty A, Chou WM, Hasreiter J, Wettengel JM, Stadler D, *et al.* Hepatitis B virus genome recycling and de novo secondary infection events maintain stable cccDNA levels. Journal of Hepatology. 2018; 69: 1231–1241. https://doi.org/10.1016/j.jhep.2018.08.012.
- [7] Ma C, Xu W, Yang Q, Liu W, Xiang Q, Chen J, et al. Osteopetrosis-Associated Transmembrane Protein 1 Recruits RNA Exosome To Restrict Hepatitis B Virus Replication. Journal of Virology. 2020; 94: e01800–19. https://doi.org/10.1128/ JVI.01800-19.
- [8] Wijaya W, Phyu SM, Jiang S. Extracellular Vesicle (EV) Survivin for Cancer Diagnostics and Therapeutics: A Review. Frontiers in bioscience (Landmark edition). 2024; 29: 302. https://doi.org/10.31083/j.fbl2908302.

- [9] Liu Z, Li Y, Wang Y, Bai X, Zhang Y. Exosomes in HBV infection. Clinica Chimica Acta; International Journal of Clinical Chemistry. 2023; 538: 65–69. https://doi.org/10.1016/j.cca. 2022.11.012.
- [10] Fusco C, De Rosa G, Spatocco I, Vitiello E, Procaccini C, Frigè C, et al. Extracellular vesicles as human therapeutics: A scoping review of the literature. Journal of Extracellular Vesicles. 2024; 13: e12433. https://doi.org/10.1002/jev2.12433.
- [11] Xu X, Zhang L, Liu J, Kong X, Yin Y, Jia Z, et al. Exosomal HBV-DNA for diagnosis and treatment monitoring of chronic hepatitis B. Open Life Sciences. 2023; 18: 20220585. https://doi.org/10.1515/biol-2022-0585.
- [12] Khabir M, Blanchet M, Angelo L, Loucif H, van Grevenynghe J, Bukong TN, et al. Exosomes as Conduits: Facilitating Hepatitis B Virus-Independent Hepatitis D Virus Transmission and Propagation in Hepatocytes. Viruses. 2024; 16: 825. https://doi.org/10.3390/v16060825.
- [13] Chu Q, Li J, Chen J, Yuan Z. HBV induced the discharge of intrinsic antiviral miRNAs in HBV-replicating hepatocytes via extracellular vesicles to facilitate its replication. The Journal of General Virology. 2022; 103: 10.1099/jgv.0.001744. https://do i.org/10.1099/jgv.0.001744.
- [14] Zeng W, Zheng L, Li Y, Yang J, Mao T, Zhang J, et al. Engineered extracellular vesicles for delivering functional Cas9/gRNA to eliminate hepatitis B virus cccDNA and integration. Emerging Microbes & Infections. 2024; 13: 2284286. https://doi.org/10.1080/22221751.2023.2284286.
- [15] Wang J, Cao D, Yang J. Exosomes in Hepatitis B Virus Transmission and Related Immune Response. The Tohoku Journal of Experimental Medicine. 2020; 252: 309–320. https://doi.org/10.1620/tjem.252.309.
- [16] Wu Q, Glitscher M, Tonnemacher S, Schollmeier A, Raupach J, Zahn T, et al. Presence of Intact Hepatitis B Virions in Exosomes. Cellular and Molecular Gastroenterology and Hepatology. 2023; 15: 237–259. https://doi.org/10.1016/j.jcmgh.2022.09.012.
- [17] Kim GW, Siddiqui A. The role of N6-methyladenosine modification in the life cycle and disease pathogenesis of hepatitis B and C viruses. Experimental & Molecular Medicine. 2021; 53: 339–345. https://doi.org/10.1038/s12276-021-00581-3.
- [18] Ge Y, Tang S, Xia T, Shi C. Research progress on the role of RNA N⁶-methyladenosine methylation in HCV infection. Virology. 2023; 582: 35–42. https://doi.org/10.1016/j.virol.2023. 03,007.
- [19] Kim GW, Siddiqui A. N6-methyladenosine modification of HCV RNA genome regulates cap-independent IRES-mediated translation via YTHDC2 recognition. Proceedings of the National Academy of Sciences of the United States of America. 2021; 118: e2022024118. https://doi.org/10.1073/pnas .2022024118.
- [20] Imam H, Khan M, Gokhale NS, McIntyre ABR, Kim GW, Jang JY, et al. N6-methyladenosine modification of hepatitis B virus RNA differentially regulates the viral life cycle. Proceedings of the National Academy of Sciences of the United States of America. 2018; 115: 8829–8834. https://doi.org/10.1073/pnas.1808319115.
- [21] Li D, Liu Y, Zhou J, Chen Y, Yang C, Liu H, et al. m6A Regulator-mediated RNA Methylation Modulates Immune Microenvironment of Hepatitis B Virus-related Acute Liver Failure. Inflammation. 2023; 46: 1777–1795. https://doi.org/10. 1007/s10753-023-01841-2.
- [22] Oerum S, Meynier V, Catala M, Tisné C. A comprehensive review of m6A/m6Am RNA methyltransferase structures. Nucleic Acids Research. 2021; 49: 7239–7255. https://doi.org/10.1093/nar/gkab378.
- [23] An Y, Duan H. The role of m6A RNA methylation in cancer



- metabolism. Molecular Cancer. 2022; 21: 14. https://doi.org/10. 1186/s12943-022-01500-4.
- [24] Ma S, Chen C, Ji X, Liu J, Zhou Q, Wang G, et al. The interplay between m6A RNA methylation and noncoding RNA in cancer. Journal of Hematology & Oncology. 2019; 12: 121. https://doi. org/10.1186/s13045-019-0805-7.
- [25] Sun L, Chen X, Zhu S, Wang J, Diao S, Liu J, et al. Decoding m⁶A mRNA methylation by reader proteins in liver diseases. Genes & Diseases. 2023; 11: 711–726. https://doi.org/10.1016/ j.gendis.2023.02.054.
- [26] Zang Q, Ju Y, Liu S, Wu S, Zhu C, Liu L, et al. The significance of m6A RNA methylation regulators in diagnosis and subtype classification of HBV-related hepatocellular carcinoma. Human Cell. 2024; 37: 752–767. https://doi.org/10.1007/s13577-024-01044-3.
- [27] Li N, Hui H, Bray B, Gonzalez GM, Zeller M, Anderson KG, et al. METTL3 regulates viral m6A RNA modification and host cell innate immune responses during SARS-CoV-2 infection. Cell Reports. 2021; 35: 109091. https://doi.org/10.1016/j.celrep.2021.109091.
- [28] Wang JN, Wang F, Ke J, Li Z, Xu CH, Yang Q, et al. Inhibition of METTL3 attenuates renal injury and inflammation by alleviating TAB3 m6A modifications via IGF2BP2-dependent mechanisms. Science Translational Medicine. 2022; 14: eabk2709. https://doi.org/10.1126/scitranslmed.abk2709.
- [29] Yu L, Zhang Z, Zeng R, Zhang J, Wang P, Pan W. METTL3 participates in m6A modification to regulate HBV replication through an IGF2BP2-dependent manner. Journal of Army Medical University. 2024; 46: 442–449. https://doi.org/10.16016/j. 2097-0927.202307062.
- [30] Oikawa R, Watanabe Y, Yotsuyanagi H, Yamamoto H, Itoh F. DNA methylation at hepatitis B virus integrants and flanking host mitochondrially encoded cytochrome C oxidase III. Oncology Letters. 2022; 24: 424. https://doi.org/10.3892/ol.2022. 13544.
- [31] Ma J, Huang C, Yao X, Shi C, Sun L, Yuan L, *et al.* Inhibition of hepatitis B virus and induction of hepatoma cell apoptosis by ASGPR-directed delivery of shRNAs. PloS One. 2012; 7: e46096. https://doi.org/10.1371/journal.pone.0046096.
- [32] Kim GW, Moon JS, Siddiqui A. N6-methyladenosine modification of the 5' epsilon structure of the HBV pregenome RNA regulates its encapsidation by the viral core protein. Proceedings of the National Academy of Sciences of the United States of America. 2022; 119: e2120485119. https://doi.org/10.1073/pnas.2120485119.
- [33] Zhang Z, Liu J, Yu L, Zeng R, Pan W. The hijacking of HBV by small extracellular vesicles inhibits M1 macrophages to facilitate immune evasion. Scientific Reports. 2024; 14: 19917. https://doi.org/10.1038/s41598-024-70924-3.
- [34] Wang X, Wei Z, Cheng B, Li J, He Y, Lan T, *et al.* Endoplasmic reticulum stress promotes HBV production by enhancing use of the autophagosome/multivesicular body axis. Hepatology (Baltimore, Md.). 2022; 75: 438–454. https://doi.org/10.1002/hep. 32178.
- [35] Ninomiya M, Inoue J, Krueger EW, Chen J, Cao H, Masamune A, *et al.* The Exosome-Associated Tetraspanin CD63 Contributes to the Efficient Assembly and Infectivity of the Hepatitis B Virus. Hepatology Communications. 2021; 5: 1238–1251. https://doi.org/10.1002/hep4.1709.
- [36] Jung S, Jacobs KFK, Shein M, Schütz AK, Mohr F, Stadler H, et al. Efficient and reproducible depletion of hepatitis B virus from plasma derived extracellular vesicles. Journal of Extracellular Vesicles. 2020; 10: e12040. https://doi.org/10.1002/jev2.12040.
- [37] Wu X, Niu J, Shi Y. Exosomes target HBV-host interactions to remodel the hepatic immune microenvironment. Journal of

- Nanobiotechnology. 2024; 22: 315. https://doi.org/10.1186/s12951-024-02544-y.
- [38] Du X, Guo Y, Zhao X, Zhang L, Fan R, Li Y. METTL3-mediated TIM1 promotes macrophage M1 polarization and inflammation through IGF2BP2-dependent manner. Journal of Biochemical and Molecular Toxicology. 2024; 38: e23845. https://doi.org/10.1002/jbt.23845.
- [39] Yi J, Peng F, Zhao J, Gong X. METTL3/IGF2BP2 axis affects the progression of colorectal cancer by regulating m6A modification of STAG3. Scientific Reports. 2023; 13: 17292. https://doi.org/10.1038/s41598-023-44379-x.
- [40] Moon JS, Lee W, Cho YH, Kim Y, Kim GW. The Significance of N6-Methyladenosine RNA Methylation in Regulating the Hepatitis B Virus Life Cycle. Journal of Microbiology and Biotechnology. 2024; 34: 233–239. https://doi.org/10.4014/jmb.2309.09013.
- [41] Liu S, Li J, Qiu M, Liu Y, Wen Q, Lin Q, et al. Genetic variants of m⁶A modification genes are associated with survival of HBV-related hepatocellular carcinoma. Journal of Cellular and Molecular Medicine. 2024; 28: e18517. https://doi.org/10.1111/jcmm.18517.
- [42] Pu J, Wang J, Qin Z, Wang A, Zhang Y, Wu X, et al. IGF2BP2 Promotes Liver Cancer Growth Through an m6A-FEN1-Dependent Mechanism. Frontiers in Oncology. 2020; 10: 578816. https://doi.org/10.3389/fonc.2020.578816.
- [43] Cheng D, Wu C, Li Y, Liu Y, Mo J, Fu L, et al. METTL3 inhibition ameliorates liver damage in mouse with hepatitis B virus-associated acute-on-chronic liver failure by regulating miR-146a-5p maturation. Biochimica et Biophysica Acta. Gene Regulatory Mechanisms. 2022; 1865: 194782. https://doi.org/10.1016/j.bbagrm.2021.194782.
- [44] Tsukuda S, Watashi K. Hepatitis B virus biology and life cycle. Antiviral Research. 2020; 182: 104925. https://doi.org/10.1016/j.antiviral.2020.104925.
- [45] Liu FY, Zhou SJ, Deng YL, Zhang ZY, Zhang EL, Wu ZB, et al. MiR-216b is involved in pathogenesis and progression of hepatocellular carcinoma through HBx-miR-216b-IGF2BP2 signaling pathway. Cell Death & Disease. 2015; 6: e1670. https://doi.org/10.1038/cddis.2015.46.
- [46] Yang Y, Wu J, Liu F, He J, Wu F, Chen J, et al. IGF2BP1 Promotes the Liver Cancer Stem Cell Phenotype by Regulating MGAT5 mRNA Stability by m6A RNA Methylation. Stem Cells and Development. 2021; 30: 1115–1125. https://doi.org/ 10.1089/scd.2021.0153.
- [47] Huang H, Weng H, Sun W, Qin X, Shi H, Wu H, et al. Publisher Correction: Recognition of RNA N⁶-methyladenosine by IGF2BP proteins enhances mRNA stability and translation. Nature Cell Biology. 2020; 22: 1288. https://doi.org/10.1038/s41556-020-00580-y.
- [48] Zhang C, Dai D, Zhang W, Yang W, Guo Y, Wei Q. Role of m6A RNA methylation in the development of hepatitis B virusassociated hepatocellular carcinoma. Journal of Gastroenterology and Hepatology. 2022; 37: 2039–2050. https://doi.org/10. 1111/jgh.15999.
- [49] Chen Y, Cai K, Du Y, Liu Z, Gong Y. HDAC1 overexpression promoted by METTL3-IGF2BP2 inhibits FGF21 expression in metabolic syndrome-related liver injury. Biochemistry and Cell Biology. 2023; 101: 52–63. https://doi.org/10.1139/bcb-2022-0314.
- [50] Zhang H, Wu D, Wang Y, Guo K, Spencer CB, Ortoga L, et al. METTL3-mediated N6-methyladenosine exacerbates ferroptosis via m6A-IGF2BP2-dependent mitochondrial metabolic reprogramming in sepsis-induced acute lung injury. Clinical and Translational Medicine. 2023; 13: e1389. https://doi.org/10.1002/ctm2.1389.

